Cumulative production of pions by heavy baryonic resonances in proton-nucleus collisions

A. Motornenko[1] and M. I. Gorenstein[2,3]

[1] *Taras Shevchenko National University of Kiev, Kiev, Ukraine*

[2] *Bogolyubov Institute for Theoretical Physics, Kiev, Ukraine*

[3] *Frankfurt Institute for Advanced Studies, Johann Wolfgang Goethe University, Frankfurt, Germany*

arXiv:1604.04308v1 [hep-ph] 14 Apr 2016

Abstract

Pion production in proton-nucleus (p+A) collisions outside the kinematical boundary of proton-nucleon (p+N) reactions, the so-called cumulative effect, is studied. Restrictions from energy-momentum conservation on the energy of pions emitted in the backward direction in the target rest frame are analyzed. It is assumed that the cumulative pions are produced in p+A reactions by heavy baryonic resonances. The baryonic resonances are first created in p+N reactions. Due to successive collisions with nuclear nucleons the masses of these resonances may then increase and, simultaneously, their longitudinal velocities decrease. We also use the Ultra relativistic Quantum Molecular Dynamics model to reveal the key role of successive collisions of baryonic resonances with nuclear nucleons for cumulative pion production in p+A reactions. Further experimental studies of cumulative hadron production in p+A reactions at high collision energies are needed to search for heavy hadron-like objects and investigate their properties.

PACS numbers: 25.75.-q, 25.75.Dw, 25.75.Ld

Keywords: proton-nucleus interactions, kinematical boundaries, UrQMD simulations

I. INTRODUCTION

About 40 years ago the so-called cumulative effect was discovered in relativistic proton-nucleus (p+A) collisions, i.e., secondary particles were detected in the kinematic region forbidden within an interaction of the projectile proton with a free nucleon [1–5]. Different theoretical models were proposed [6–23], however, a physical origin of this effect is still not settled. In the present paper the cumulative effect is considered for pion production in inclusive reactions p+A$\to \pi(180^\circ) + X$ with the pion emitted at 180°, i.e., in the backward direction in the rest frame of nuclei A. First experiments on cumulative particle production [1–3] were performed at Synchrophasotron accelerator of the Joint Institute for Nuclear Research in Dubna. The momenta of projectile protons were taken as $p_0 = 6$ GeV/c and 8.4 GeV/c. The p+A reactions with $p_0 = 400$ GeV/c were then studied [4, 5] at Fermilab, USA. In both experiments atomic numbers of nuclear target were varied in a wide region $A = 10 \div 200$.

Let E_π^* denotes the maximal possible energy of the pion emitted at angle 180° in the laboratory frame in a proton-nucleon (p+N) interaction at fixed projectile proton momentum p_0. In p+A collisions at the same projectile proton momentum p_0, pions emitted at 180° in the laboratory frame (this frame coincides with the nucleus rest frame) with energies $E_\pi > E_\pi^*$, even above $2E_\pi^*$, were experimentally observed [1–5].

The results of Ref. [6] demonstrated that Fermi motion of nuclear nucleons can not describe the data of the cumulative pion production. In Ref. [7] a fireball model of cumulative effect was proposed. According to that model, particle production in the cumulative region $E_\pi > E_\pi^*$ is due to the formation of a massive hadronic fireball, successive collisions of this fireball with nuclear nucleons, and finally its decay with emission of a cumulative particle. In the present paper we critically analyze the main assumptions of that approach. We clarify the basic restrictions on the energy E_π for the backward pion production in p+N and p+A reactions. These are restrictions that follow from energy-momentum conservation.

Particle production in most phenomenological models, e.g., in the popular relativistic transport models – Ultra relativistic Quantum Molecular Dynamics (UrQMD) [24] and Hadron String Dynamics (HSD) [25] – takes place exclusively by means of binary reactions,

$$h_1 \ + \ h_2 \ \to \ H_1 \ + \ H_2 \ , \tag{1}$$

with subsequent decays of H_1 and/or H_2 excited states. These reactions satisfy energy-momentum conservation, as well as conservations of baryonic number, electric charge, and strangeness. In elementary particle collisions, like p+N, the excited states H_1 and/or H_2 are hadronic resonances and/or strings, while h_1 and h_2 are stable hadrons. In p+A and A+A col-

lisions, h_1 or/and h_2 can be also resonance(s), and H_1 or/and H_2 can be the stable hadron(s). Therefore, any relations between masses of h_1, h_2 and H_1, H_2 in Eq. (1) are possible in the course of p+A and A+A reactions. Among secondary inelastic reactions there are also the following

$$h_1 \ + \ h_2 \ \rightarrow \ H \ , \tag{2}$$

where h_1 and h_2 can be both mesons, baryon and antibaryon (H is the meson resonance or mesonic string in these cases), or meson and baryon (H is the baryonic resonance or baryonic string). Experimental information on the quantum numbers and decay channels of mesonic and baryonic resonances is available, and the string model [26] is assumed to describe the formation and decay of strings.

The main physical quantities in our analysis are the masses and longitudinal (i.e. along the collision axis) velocities of the baryonic resonances created in reactions (1). In p+A collisions, resonances R are first produced in p+N$\rightarrow$ R+N reactions, and later they participate in successive R+N$\rightarrow$ R'+N collisions. The evolution of these quantities due to subsequent collisions of the resonances with nuclear nucleons in the course of p+A reaction is investigated. It is argued that the cumulative pions in p+A reactions are created by baryonic resonances with very high masses that are formed due to successive collisions with nuclear nucleons. We also use the UrQMD model to describe the existing data and analyze some microscopic aspects of cumulative pion production in p+A reactions.

The paper is organized as follows. In Sec. II the basic restrictions from relativistic kinematics on pion production in p+N reactions are considered. In Sec. III the kinematic restrictions on pion production in p+A collisions are discussed. The role of successive collisions of a baryonic resonance created in p+N reaction with other nucleons inside the nucleus target is investigated. In Sec. IV the UrQMD model is applied to backward pion production in p+p and p+A reactions. A summary in Sec. V closes the article.

II. KINEMATIC RESTRICTIONS IN N+N REACTIONS

In this section we consider general restrictions on energy E_π of the pion emitted in the backward direction (i.e., at 180°) in p+N reactions in the target rest frame. These restrictions are consequences of the energy-momentum conservation. We are interested in finding a maximal value of the pion energy. Two nucleons should be anyhow present in a final state because of baryonic number conservation. It is evident that the production of any additional hadron(s)

and/or a presence of non-zero transverse momenta in the final state of two nucleons would require an additional energy and lead to a reduction of E_π value at fixed projectile momentum p_0. Thus, to find the maximum of E_π one should consider only the reaction p+N$\to$ $\pi(180^\circ)$+N+N and restrict the kinematical analysis to the one-dimensional (longitudinal) direction, i.e., all particle momenta should be directed along the collision axis. The emission of π-meson at 180° is mediated by a baryonic resonance state. Different stages of the NN$\to$NN$\pi(180^\circ)$ reaction are schematically presented in Fig. 1.

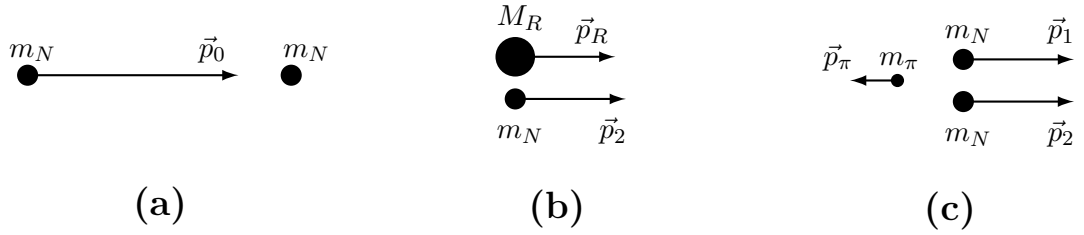

Figure 1: Pion production in NN$\to$NN$\pi(180^\circ)$ reaction. (a): initial stage. (b): intermediate stage. (c): final stage.

The energy-momentum conservation in the target rest frame reads[1]:

$$\sqrt{p_0^2+m_N^2}+m_N=\sqrt{p_\pi^2+m_\pi^2}+\sqrt{p_1^2+m_N^2}+\sqrt{p_2^2+m_N^2}\ , \qquad p_0=p_1+p_2-p_\pi\ , \quad (3)$$

where p_1 and p_2 are absolute values of the final state nucleon momenta, and $p_\pi=\sqrt{(E_\pi)^2-m_\pi^2}$ is that of the pion emitted in the backward direction. Substituting p_2 from the second equation of Eq. (3) to the first one the value of E_π is presented as a function of p_0 and p_1. At fixed p_0, the pion energy E_π reaches its maximal value denoted as E_π^* at the point where $\partial E_\pi/\partial p_1=0$. One finds

$$p_1^*\equiv p_1=p_2=\frac{p_0+p_\pi^*}{2}\ , \quad (4)$$

thus, both nucleons should have the same values of final momenta. The maximal pion energy is then given by an implicit equation[2]

$$E_\pi^*=m_N+\sqrt{m_N^2+p_0^2}-2\sqrt{m_N^2+\left(\frac{p_0+\sqrt{(E_\pi^*)^2-m_\pi^2}}{2}\right)^2}\ . \quad (5)$$

[1] We use values t he $m_N\cong 0.94$ GeV/c^2 and $m_\pi\cong 0.14$ GeV/c^2 for the nucleon and pion masses, respectively, neglecting small mass differences for different isospin states.

[2] Equation (5) can be transformed to a 4th order algebraic equation. Its explicit solution is, however, too cumbersome and gives no advantages.

The index 1 in p_1^* (also in M_1^* and v_1^* below) reminds that these quantities are obtained in a collision of the projectile proton with *one* nucleon. The solution of Eq. (5) for E_π^* is presented in Fig. 2 as a function of p_0.

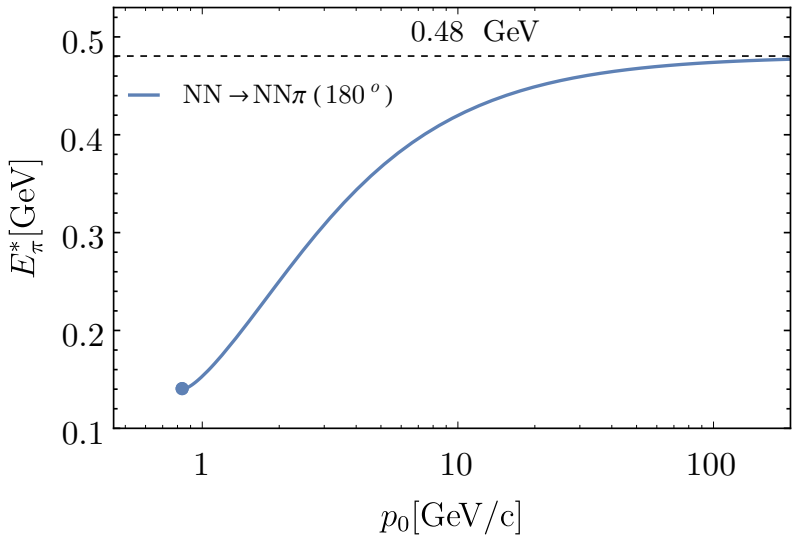

Figure 2: The maximal pion energy E_π^* in NN→NNπ(180°) reaction presented in Fig. 1. E_π^* is calculated from Eq. (5) as a function of projectile proton momentum p_0. A threshold value $p_0 \cong 0.83$ GeV/c corresponds to $p_\pi = 0$. Horizontal dashed line presents the upper limit for E_π^* at $p_0 \to \infty$.

A minimal (threshold) value of $p_0 \cong 0.83$ GeV/c is needed to create a pion with $p_\pi = 0$. For $p_0 > 0.83$ GeV/c the backward pion production with non-zero momenta p_π becomes possible. As seen from Fig. 2 the value of E_π^* increases monotonously with p_0, and approaches its upper limit $(m_N^2 + m_\pi^2)/(2m_N) \cong 0.48$ GeV at $p_0 \to \infty$. Note that for $p_0 = 6$ GeV/c and 8.4 GeV/c used in p+A experiments [1] maximal values of the pion energy in p+N reactions are equal to $E_\pi^* \cong 0.38$ GeV and 0.41 GeV, respectively. These values are about two times smaller than those observed in the p+A data [1]. From Fig. 2 it also follows that at large p_0, the value of E_π^* becomes insensitive to p_0. Therefore, the production of additional pions with not too large *positive* longitudinal momenta has small influence on the E_π^* value.

The invariant mass M_1^* and velocity v_1^* of the resonance R that decays into $\pi(180°)$ with maximal energy E_π^* can be calculated as

$$M_1^* = \left[\left(\sqrt{m_N^2 + (p_1^*)^2} + E_\pi^* \right)^2 - (p_1^* - p_\pi^*)^2 \right]^{1/2}, \quad v_1^* = \left[1 - \frac{(M_1^*)^2}{(M_1^*)^2 + (p_1^* - p_\pi^*)^2} \right]^{1/2}, \quad (6)$$

and they are presented as functions of p_0 in Figs. 3 (a) and (b), respectively. We use the subscript 1 to denote the M^* and v^* values resulting from *single* p+N collision.

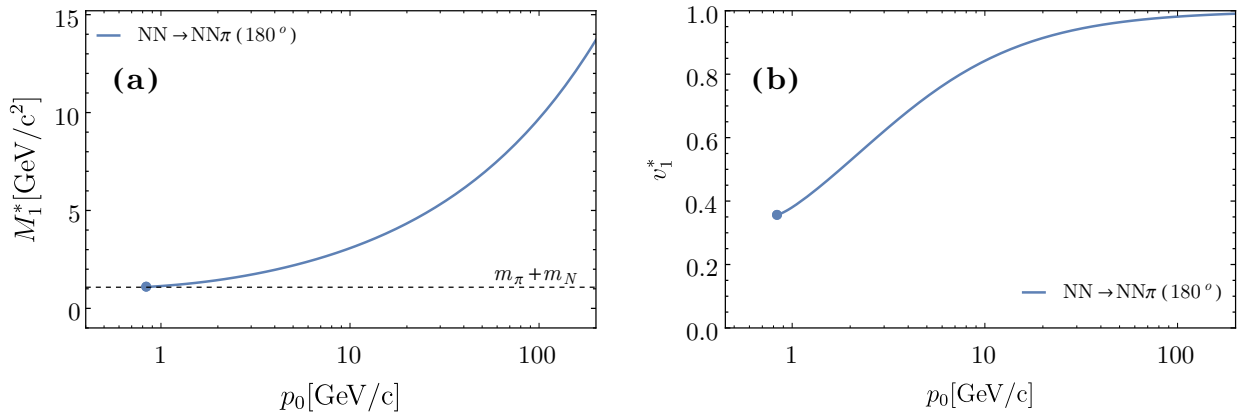

Figure 3: Invariant mass M_1^* (a) and longitudinal velocity v_1^* (b) of resonance R from Fig. 1 (b) that decays into $\pi(180°)$ with maximal energy E_π^*. M_1^* and v_1^* are calculated from Eq. (6) as functions of p_0.

From Fig. 3 (a) it is seen that M_1^* increases monotonously with p_0, and $M_1^* \cong \sqrt{m_N p_0}$ at $p_0 \to \infty$. Particularly, at $p_0 \geq 20$ GeV/c one finds $M_1^* \geq 4.3$ GeV/c^2. Thus, an evident question arises: what is the physical origin of these massive systems? Or, in other words, what is the microscopic mechanism of a production of pions at 180° with energy E_π^* in p+N reactions at large p_0. In most relativistic transport models the objects that are responsible for the production of new hadrons can be either resonances or strings. In what follows we use a common notation, resonance, for these objects and will return to the discussion of their physical meaning in Sec. IV.

In a baryonic resonance decay, $R \to \mathrm{N} + \pi(180°)$, the value of E_π depends on the resonance mass M_R and its longitudinal velocity v_R. In the resonance rest frame the pion energy and momentum can be easily found

$$E_\pi^0 = \frac{M_R^2 - m_N^2 + m_\pi^2}{2M_R}\ , \qquad p_\pi^0 = \sqrt{(E_\pi^0)^2 - m_\pi^2}\ . \tag{7}$$

The energy E_π, in the laboratory frame, is obtained as

$$E_\pi = \frac{E_\pi^0 - v_R p_\pi^0}{\sqrt{1 - v_R^2}}\ . \tag{8}$$

Therefore, both the increase of M_R and decrease of v_R provide an extension of the available kinematic region of E_π for pions emitted at 180°. This is most clearly seen if one neglects the pion mass, i.e., for $E_\pi^0 \cong p_\pi^0$ (this is valid at $M_R \gg m_N$). One then obtains

$$E_\pi \cong E_\pi^0 \sqrt{\frac{1 - v_R}{1 + v_R}}\ . \tag{9}$$

Thus, the suppression of E_π compared to E_π^0 can be interpreted as Doppler effect ("red shift" effect).

Let us consider the possible values of M_R and v_R admitted by relativistic kinematics in reaction p+N$\to$ R+N (see Fig. 1) at fixed p_0. As before, all particle momenta are assumed to be directed along the collision axis. From the energy-momentum conservation,

$$\sqrt{m_N^2+p_0}+m_N=\sqrt{M_R^2+p_R^2}+\sqrt{m_N^2+p_N^2}\ , \qquad p_0=p_R+p_N\ , \tag{10}$$

one finds

$$M_R^2=m_N^2+2p_0p_N-2\left(\sqrt{m_N^2+p_0^2}+m_N\right)\left(\sqrt{m_N^2+p_N^2}-m_N\right)\ , \tag{11}$$

$$v_R=\sqrt{1\ -\ \frac{M_R^2}{M_R^2+p_R^2}}\ . \tag{12}$$

The resonance mass M_R (11) and velocity v_R (12) are shown in Figs. 4 (a) and (b), respectively, as functions of p_N at fixed $p_0=6$ GeV/c .

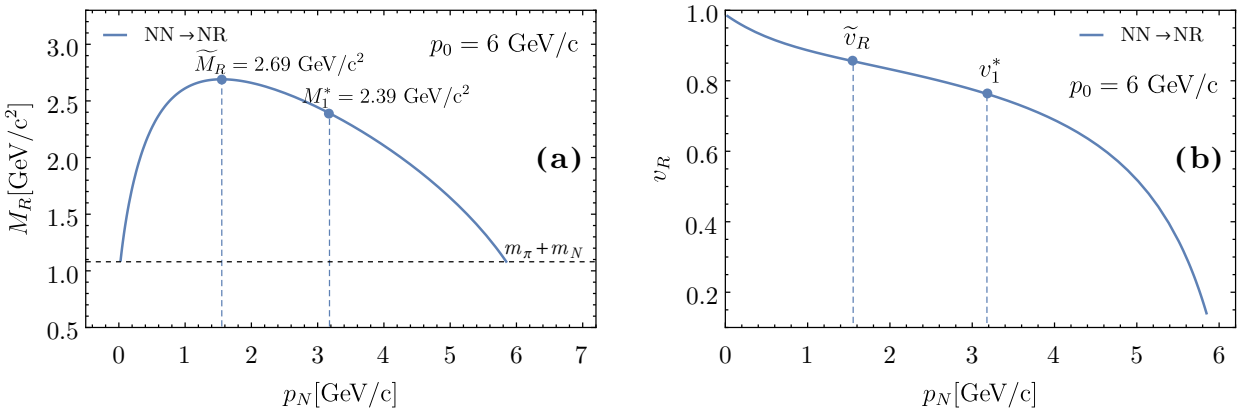

Figure 4: Resonance mass M_R (a) and longitudinal velocity v_R (b) that are possible in NN$\to$NN$\pi(180^\circ)$ reactions presented in Fig. 1 (b). M_R and v_R are calculated from Eq. (11) and Eq. (12), respectively, as functions of p_N at fixed $p_0=6$ GeV/c.

The maximum value of $M_R=\tilde{M}_R$ found from Eq. (11) at fixed p_0 corresponds the condition $\partial M/\partial p_N=0$ that gives

$$\tilde{p}_N\equiv\sqrt{\frac{m_N}{2}\left(\sqrt{m_N^2+p_0^2}-m_N\right)}\ . \tag{13}$$

Note that Eq. (13) is equivalent to the condition that the resonance with mass M_R and nucleon move with the same velocities, both equal to v_R. It should be noted that the nucleon momenta $\tilde{p}_N$ given by Eq. (13) is smaller than the value of $p_1^*=(p_0+p_\pi^*)/2$ given by Eq. (4) and required

to obtain $E_\pi = E_\pi^*$. One then finds that $\tilde{M}_R$ obtained from Eqs. (11) and (13) is larger than the invariant mass M_1^* given by Eq. (6) that is needed to emit $\pi(180^\circ)$ with maximal energy E_π^*.

One might intuitively expect that maximal energy of $\pi(180^\circ)$ should correspond to a maximal mass $\tilde{M}_R$ of an intermediate resonance. This is because larger value of mass M_R leads to a larger value of the pion energy in its *rest frame* as given by Eq. (7). Moreover, a naive expectation might be that a resonance with a larger value of M_R should move with a slower velocity v_R that makes $E_\pi(180^\circ)$ yet larger. These intuitive expectations are, however, not correct. Conservation of both the energy and momentum leads to the non-trivial connection between M_R and v_R values. As seen from Fig. 4 (b), v_R decreases monotonously with p_N. Thus, the largest mass $\tilde{M}_R$ does not correspond to the smallest velocity v_R. On the other hand, too small velocity v_R would correspond to too small resonance mass M_R, and the backward production of cumulative pions would become impossible. To emit a π-meson at 180° with $E_\pi = E_\pi^*$ a compromise between large M_R and small v_R should be found, i.e., the value of E_π (8) should be maximized. These *optimal* values of M_R and v_R are just M_1^* and v_1^*, respectively. A comparison of M_1^* with $\tilde{M}_R$ and v^* with $\tilde{v}_R$ as functions of p_0 is presented in Fig. 5 (a) and (b), respectively.

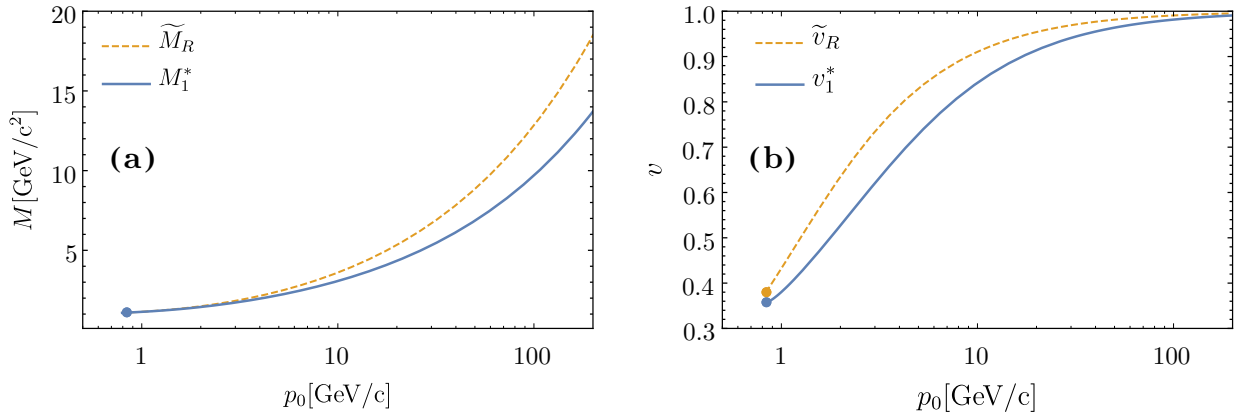

Figure 5: (a): Invariant mass M_1^* given by Eq. (6) and $\tilde{M}_R$ given by Eqs. (11) and (13) are presented as functions of p_0 by solid and dashed line, respectively. (b): Velocity v_1^* (6) and $\tilde{v}_R$ (12,13) are shown as functions of p_0 by solid and dashed line, respectively. Values M_1^* and v_1^* provide the maximal energy E_π^* of $\pi(180^\circ)$. $\tilde{M}$ and $\tilde{v}_R$ provide the maximal mass of intermediate resonance R in the reaction shown in Fig. 1 (b).

III. SUCCESSIVE COLLISIONS WITH NUCLEAR NUCLEONS

As shown in the previous section, an energy of the pion emitted at 180° in p+N reactions is restricted by the E_π^* value presented in Fig. 2 as a function of p_0. However, pion energies even larger than $2E_\pi^*$ were observed experimentally in p+A collisions [1, 2]. One therefore should admit that the production of cumulative pions in p+A collisions involves more than one target nucleon.

A multi-nucleon system inside a nucleus can manifest itself in various ways. For example, inter-nucleon interactions in a nucleus may lead to one-particle momentum distribution with a long tail (see Refs. [8–11]). Another possibility to create particles beyond the kinematical boundary allowed in p+N reactions is to assume that a projectile proton interacts in an individual collision simultaneously with a multi-nucleon system, the so-called "grain" or "flucton" (see Ref. [2, 6]). Indeed, if the target mass equals $2m_N$, $3m_N$, etc., cumulative particle production may take place. Both these approaches refer to some uncommon aspects of nuclear physics. An object responsible for the cumulative particle production is assumed to exist inside a nucleus prior to its collision with a projectile. Interpretation of these objects as multi-quark states and calculations based on parton distribution functions were discussed in Refs. [6, 12–14].

In the present study we will advocate the approach suggested in [7], see also Refs. [15–19]. It assumes that instead of a large mass of multi-nucleon target, cumulative particle production takes place due to the large mass of the projectile baryonic resonance created in the *first* p+N collision and propagated further through the nucleus. This baryonic resonance has a chance to interact with other nuclear nucleons earlier than it decays to free final hadrons. As we will demonstrate in this section the *successive collisions* of the baryonic resonance with nuclear nucleons may both enlarge M_R and, simultaneously, reduce v_R values in comparison to their M_1^* and v_1^* values given by Eq. (6). As seen from Eq. (8), both effects lead to larger values of E_π and, thus, extend the kinematic region for cumulative pion production. In contrast to the "grain" model, the object responsible for the cumulative production of $\pi(180^\circ)$, i.e., the heavy and slow moving resonance, does not exist inside a nucleus but is formed during the whole evolution process of p+A reaction. Note that the role of rescattering effects in cumulative hadron production were also discussed in Refs. [20–22].

Let us consider successive collisions with nuclear nucleons: p+N $\to R_1$+N, R_1+N $\to R_2$+N, *etc.* It is assumed that after n-th collision the baryonic resonance decays, $R_n \to \pi(180^\circ)$ + N.

The energy and momentum conservation between initial and final state read as

$$\sqrt{m_N^2+p_0^2}+n\,m_N=\sum_{i=1}^{n+1}\sqrt{m_N^2+p_i^2}+E_\pi\ ,\qquad p_0=\sum_{i=1}^{n+1}p_i-p_\pi\ . \tag{14}$$

The maximal pion energy E_π after n successive collisions denoted now $E^*_{\pi,n}$ can be found from Eq. (14) using the extremum conditions $\partial E_\pi/\partial p_i=0$. This leads to

$$p^*_{N,n}\equiv p_1=p_2=...=p_{n+1}=\frac{p_0+p^*_{\pi,n}}{n+1}\ , \tag{15}$$

and gives an implicit equation for $E^*_{\pi,n}$

$$E^*_{\pi,n}=n\,m_N+\sqrt{m_N^2+p_0^2}-(n+1)\sqrt{m_N^2+\left(\frac{p_0+\sqrt{(E^*_{\pi,n})^2-m_\pi^2}}{n+1}\right)^2}\ . \tag{16}$$

The maximal energies $E^*_{\pi,n}$ of pions emitted at 180° are presented in Fig. 6.

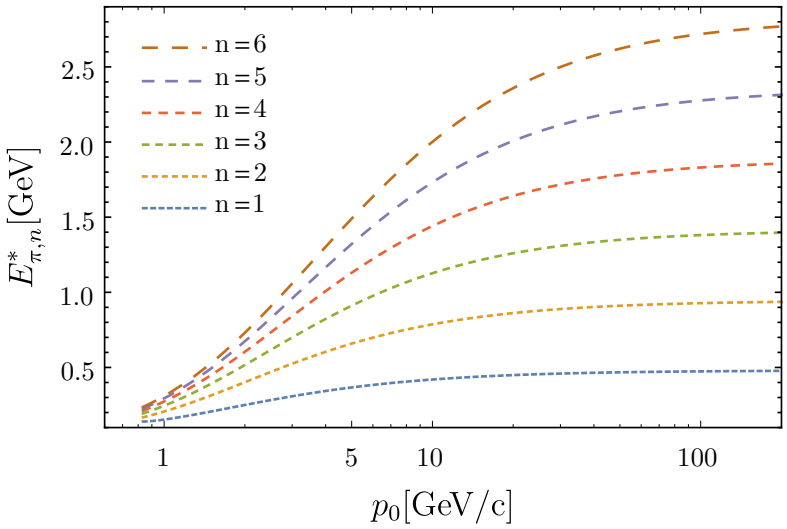

Figure 6: Maximal energies $E^*_{\pi,n}$ (16) of π-meson emitted at 180° after n successive collisions with nuclear nucleons ($n=1,\ldots,6$) as functions of projectile proton momentum p_0.

Note that for $n=1$ Eqs. (15) and (16) are reduced to Eqs. (4) and (5), respectively, i.e., $E^*_{\pi,1}\equiv E^*_\pi$ which is also shown in Fig. 2. As seen from Fig. 6, the value of maximum pion energy $E^*_{\pi,n}$ in the backward direction increases essentially with the number of collisions n. Besides, at any n, the value of $E^*_{\pi,n}$ increases monotonously with p_0, and at $p_0\to\infty$ it goes to the upper limits $n(m_N^2+m_\pi^2/n^2)/(2m_N)\cong n\cdot 0.48$ GeV, i.e., $E^*_{\pi,n}$ increases approximately linearly with the number of collisions at $p_0\to\infty$.

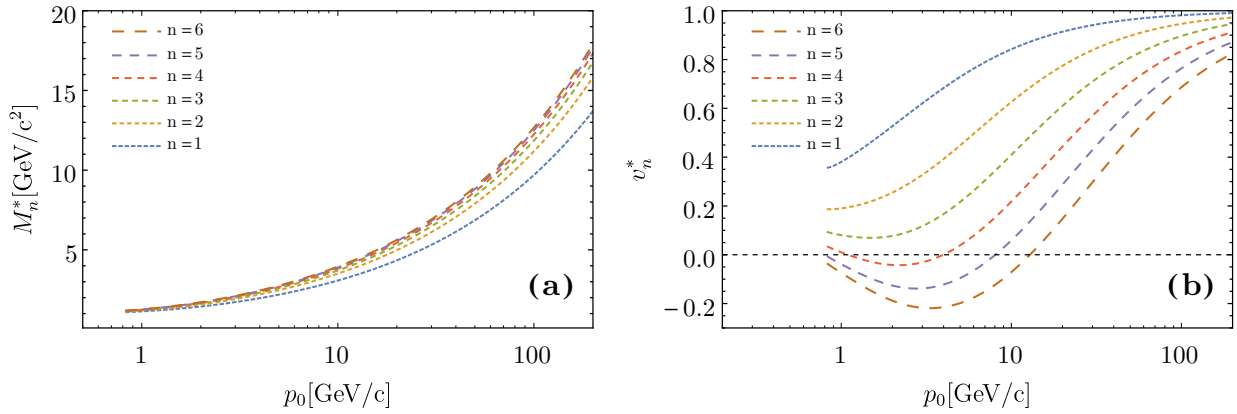

Figure 7: Invariant masses M_n^* (a) and velocities v_n^* (b) of the baryonic resonances after n successive collisions with nuclear nucleons. The values of M_n^* and v_n^* are required to provide the maximal energy $E_{\pi,n}^*$ of $\pi(180^\circ)$. They are calculated from (17) and (18), respectively, as functions of projectile proton momentum p_0.

The invariant mass M_n^* and longitudinal velocity v_n^* of the resonance after n successive collisions with nuclear nucleons are given by the same formulae as in Eq. (6) but with a substitution of p_1^* (4) by p_n^* (15)

$$M_n^* = \left[\left(\sqrt{m_N^2 + (p_n^*)^2} + E_{\pi,n}^*\right)^2 - \left(p_{N,n}^* - p_{\pi,n}^*\right)^2\right]^{1/2}, \tag{17}$$

$$|v_n^*| = \left[1 - \frac{(M_n^*)^2}{(M_n^*)^2 + (p_{N,n}^* - p_{\pi,n}^*)^2}\right]^{1/2}. \tag{18}$$

These quantities as functions of p_0 are presented in Fig. 7 for $n = 1, \ldots, 6$.

Note also that Eqs. (15) and (16) can be interpreted as a collision of the projectile proton with the n-nucleon "grain", i.e., the resulting conservation laws for the cumulative production of $\pi(180^\circ)$ with $E_\pi = E_{\pi,n}^*$ due to successive collisions with n nucleons look the same as in a collision with the n-nucleon "grain".

From Fig. 7 one sees that M_n^* increases with p_0 and $M_n^* \cong \left(\frac{2n}{n+1} m_N p_0\right)^{1/2}$ at $p_0 \to \infty$. Besides, the mass M_n^* increases monotonously and velocity v_n^* decreases monotonously with the number of collisions n at each p_0. Note that M_n^* demonstrates only a modest increase with n. Thus, the increase of $E_{\pi,n}^*$ with n seen in Fig. 6 takes place mainly due to a noticeable decrease of v_n^* as it is seen from Fig. 7 (b).

A surprising behavior with $v_n^* < 0$ for $n \geq 4$ is observed at some finite regions of projectile momentum p_0, i.e., heavy resonance may start to move backward after a large number of successive collisions for not too large p_0. In p+N$\to$ R+N reactions the only v_R values with

$v_R > 0$ are permitted. This was tacitely assumed in Eqs. (8) and (9). However, Eqs. (8) and (9) remain also valid for $v_R < 0$. In contrast to the case when E_π is reduced due to $v_R > 0$, the $v_R < 0$ values lead to enhancement of E_π. Particularly, Eq. (9) exhibits the "blue shift" of the $\pi(180^\circ)$ energy at $v_R < 0$.

Let us look at the evolution of the resonance mass and its velocity due to successive collisions with nuclear nucleons, namely, how the values of M_R and v_R should evolve after each kth collisions ($k = 1, \ldots, n$) to reach their final values M_n^* and v_n^* after the nth collision. We calculate the masses $M_{n,k}^*$ and velocities $v_{n,k}^*$ of the resonance after each of n successive collisions, $k = 1, \ldots, n$. The corresponding masses $M_{n,k}^*$ and velocities $v_{n,k}^*$ are presented in Fig. 8 (a) and (b), respectively, as functions of $k = 1, \ldots, n$ for different $n = 1, \ldots, 8$, and at fixed $p_0 = 6$ GeV/c. Note that $M_{n,n} \equiv M_n^*$ and $v_{n,n} \equiv v_n^*$, and these quantities are shown in Figs. 7 (a) and (b), respectively.

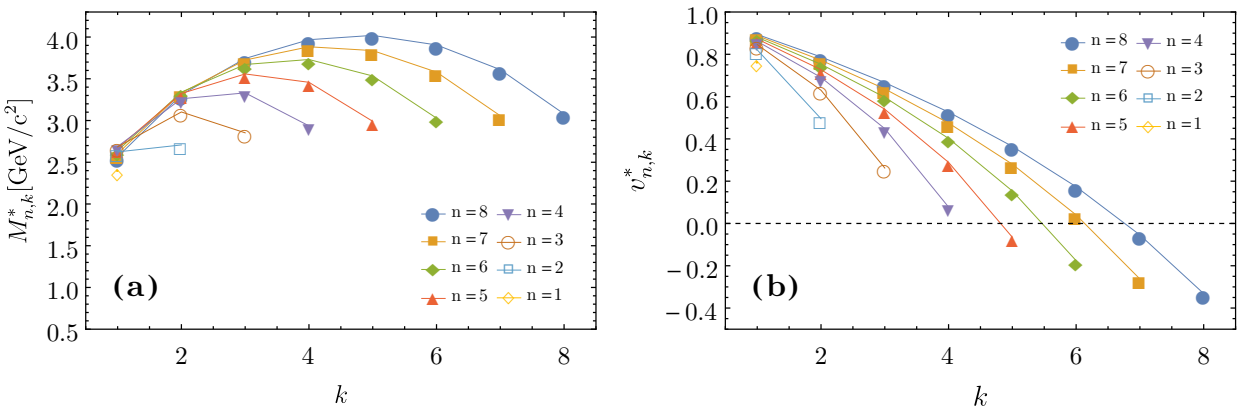

Figure 8: Mass of resonance $M_{n,k}^*$ (a) and its velocity $v_{n,k}^*$ (b) for k-th collision $k = 1, \ldots, n$ of total $n = 1, \ldots, 8$ at fixed $p_0 = 6$ GeV/c.

One sees from Fig. 8 (a) that at $k \approx n/2$ the mass $M_{n,k}^*$ reaches its maximum and starts to decrease at $k \geq n/2$ in each subsequent collision. On the other hand, the resonance velocity decreases monotonously after each subsequent collision and may become negative at large k.

We demonstrate now explicitly that a massive particle (resonance) may change its motion in backward direction after a collision with a lighter particle (nucleon) at rest. This is schematically shown in Fig. 9.

This is only possible due to the relativistic kinematics which admits the changes of particle masses in a course of the reaction. Let us consider the reaction $R + \mathrm{N} \to R' + \mathrm{N}$. The conservation laws for this reaction look similar to Eq. (10)

$$\sqrt{M_R^2 + p_R^2} + m_N = \sqrt{M_{R'}^2 + p_{R'}^2} + \sqrt{m_N^2 + p_N^2}\ , \qquad p_R = p_{R'} + p_N\ , \tag{19}$$

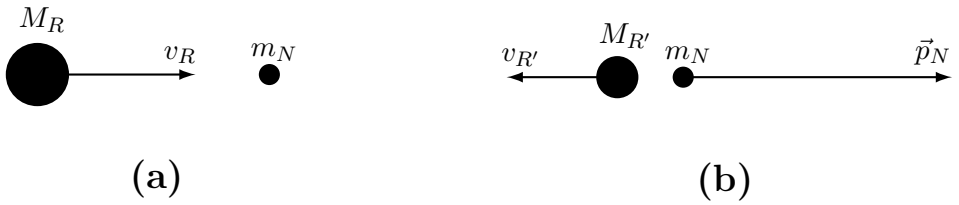

Figure 9: R+N→ R'+N reaction. (a): initial stage. (b): final stage.

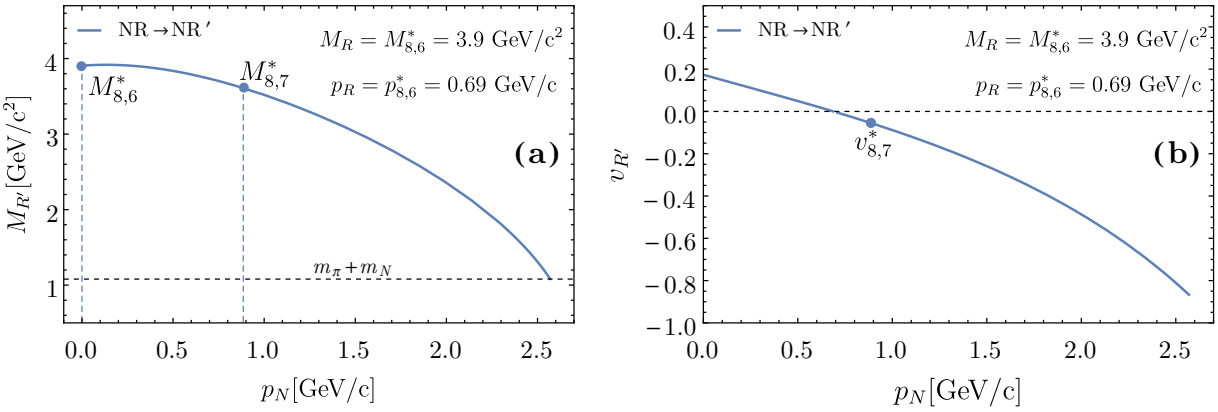

Figure 10: The resonance mass $M_{R'}$ (a) given by Eq. (19) and its velocity $v_{R'}$ (b) for reaction on Fig. 9 calculated at $M_R = M^*_{8,6} = 3.9$ GeV/c^2 and $v_R = v^*_{8,6} = 0.17$.

but the projectile mass is now $M_R > m_N$. To be definite, we take the values of $M_R = M^*_{8,6} = 3.9$ GeV/c^2 and $v_R = v^*_{8,6} = 0.17$ shown in Fig. 8. The possible values of $M_{R'}$ and $v_{R'}$ as functions of p_N are shown in Figs. 10 (a) and (b), respectively.

It can be easily seen from Fig. 10 that negative values $v_{R'} < 0$ become indeed possible, but only if the resonance loses its mass, i.e., $M_{R'} < M_R$, in a collision with a nucleon.

Taking initial values in Eq. (19) as $M_R = M^*_{8,7} = 3.61$ GeV/c^2 and $v_R = v^*_{8,7} = -0.05$ one finds another unexpected possibility shown schematically in Fig. 11. In this case, the possible

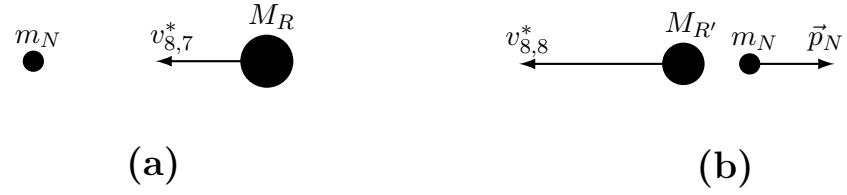

Figure 11: R+N→ R'+N reaction. (a): initial stage. (b): final stage.

values of $M_{R'}$ and $v_{R'}$ as functions of p_N are shown in Figs. 12 (a) and (b), respectively.

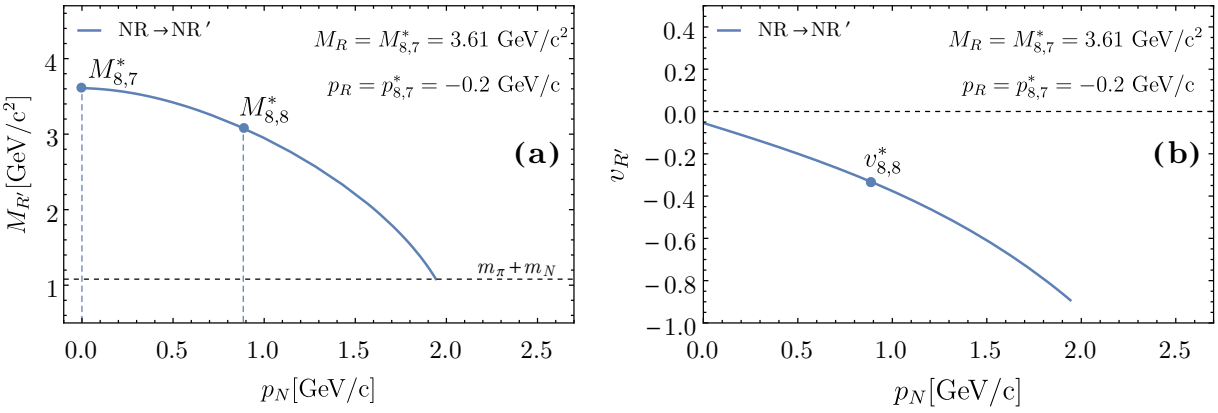

Figure 12: The resonance mass $M_{R'}$ (a) given by Eq. (19) and its velocity $v_{R'}$ (b) for reaction on Fig. 11 calculated at $M_R = M^*_{8,7} = 3.61$ GeV/c^2 and $v_R = v^*_{8,7} = -0.05$.

It should be noted that the values of M^*_n and v^*_n found in this section are by no means typical (or average) ones. In fact, the probability to reach these values in p+A reaction is very small. In other words, cumulative pion production is a very rare process.

IV. URQMD SIMULATIONS

In the present section we analyze the cumulative production of $\pi(180^\circ)$ within the UrQMD model [24]. The UrQMD is a microscopic transport model used to simulate relativistic heavy ion collisions in a wide range of collision energies. The version UrQMD-3.4 is used in the present study. There are two distinct sources of particle production in the UrQMD: formation and decays of resonances and formation and decays of hadronic strings. Most important resonances for the cumulative pion production are the baryonic resonances $N^* = (N^0, N^+)$ and $\Delta = (\Delta^-, \Delta^0, \Delta^+, \Delta^{++})$. With increasing of p_0 the excitations of baryonic strings open the new channels of hadron production in p+N reactions. At projectile momenta $p_0 \geq 18$ GeV/c the string production dominates in the UrQMD description of the inelastic p+N cross section [24].

All type of binary collisions (1), particularly $R + \mathrm{N} \to R' + \mathrm{N}$, considered in the previous sections are possible in the UrQMD model. The UrQMD has an upper limit for the mean resonance mass (this limit is different in different versions of he model). However, due to continuous Breit-Wigner mass distribution quite big resonance masses may appear. The masses of the strings are not restricted. On the other hand, in the UrQMD, as well as in other relativistic transport model, the reactions String $+ h \to X$ are not permitted. This means that, in contrast to resonances, strings can not participate in secondary reactions as real objects, only their decay products can take place in successive reactions.

A. UrQMD simulation of p+p reactions

First, we make the UrQMD analysis for p+p→ $\pi(180°)$+X reactions at p_0 =6 GeV/c and 158 GeV/c. In p+p and p+A reactions we define the backward pions as those with $\theta = 180° \pm 6°$ in the target rest frame. In Fig. 13 the energy spectra of pions in reactions p+p→ $\pi(180°) + X$ are presented at p_0 = 6 GeV/c (a) and (b) and at p_0 = 158 GeV/c (c) and (d). In Fig. 13

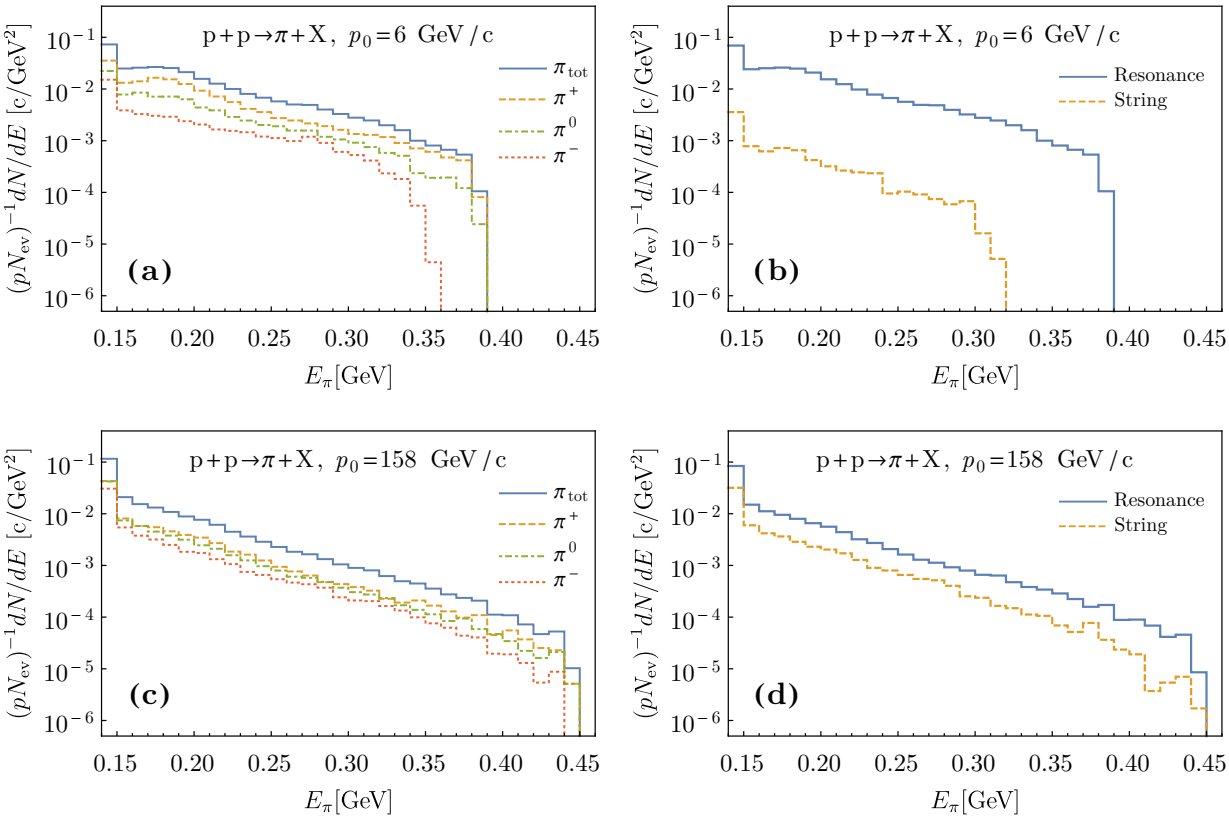

Figure 13: UrQMD results for the pion energy spectra at 180° in p+p collisions. (a): The spectra of π^+, π^0, and π^- at $p_0 = 6$ GeV/c. The number of events $N_{\rm ev} = 7 \cdot 10^7$. (b): The solid line presents the total pion spectrum from resonance decays, the dashed line – from the decay of strings. $p_0 = 6$ GeV/c, $N_{\rm ev} = 7 \cdot 10^7$. (c): Same as in (a) but at $p_0 = 158$ GeV/c, $N_{\rm ev} = 1.4 \cdot 10^8$. (d): Same as in (b) but at $p_0 = 158$ GeV/c, $N_{\rm ev} = 1.4 \cdot 10^8$.

(a) and (c) the energy spectra of π^+, π^0, and π^- are presented at p_0 = 6 GeV/c and p_0 = 158 GeV/c, respectively. As seen from Fig. 13 (a) the largest energy E_π for π^+ and π^0 reaches the maximal possible value E^*_π = 0.38 GeV for p_0=6 GeV/c (see Fig. 2). These pions are produced in reactions p+p→p+n+π^+ and p+p→p+p+π^0. The mass of intermediate baryonic resonance needed for $\pi(180°)$ production with energy $E^*_\pi = 0.38$ GeV is $M_R \cong 2.4$ GeV/c^2 (see Fig. 3 (a)). The number of produced π^- in the backward direction is smaller than that of π^+.

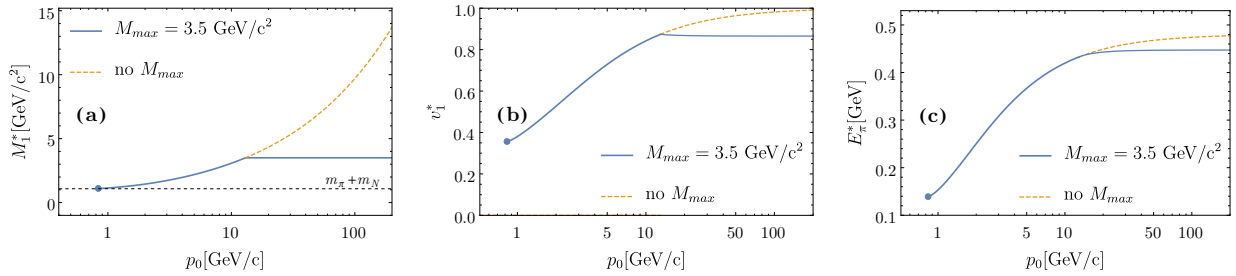

Figure 14: Mass of intermediate resonance M_R (a), its longitudinal velocity v_R (b), and maximal energy $E_\pi^{\max}$ of $\pi(180°)$ (c) as functions of p_0. The upper limit for resonance mass is fixed as $M_{\max}$=3.5 GeV/c^2. The dashed lines correspond to M_1^*, v_1^*, and E_π^* shown in Figs. 3 and 2.

Besides, the maximal value of E_{π^-} is noticeably smaller than $E_\pi^* = 0.38$ GeV. This is because one needs to produce at least one extra π^+, i.e., p+p→p+p+$\pi^+ + \pi^-$, to satisfy the electric charge conservation. Figure 13 (b) shows the contributions from resonances (solid line) and strings (dashed line) to the total pion energy spectrum at 180°, i.e., to the sum over all isospin states shown in Fig. 13 (a). The contribution from string is essentially smaller than that from resonances, and the maximal possible pion energy $E_\pi^* = 0.38$ GeV is not reached. This is because the two baryonic strings are excited in a collision of two baryons. As a consequence, at least *two* pions should be emitted in the decay of both strings.

Figures 13 (c) and (d) present the UrQMD results in p+p reactions at p_0=158 GeV/c. The difference between π^+ and π^- spectra becomes smaller, and the maximal pion energy $E_\pi^{\max} \cong 0.45$ GeV is approximately the same. This $E_\pi^{\max}$ energy is smaller than $E_\pi^* = 0.48$ GeV seen in Fig. 2. To reach the pion energy $E_\pi^* = 0.48$ GeV the mass of intermediate baryonic resonance needed should be $M_R \cong$12.2 GeV/c^2 (see Fig. 3 (a)). However, in the UrQMD there are no resonances with such large masses.

Let us find the value of maximum energy for $\pi(180°)$ when there is an upper limit for intermediate resonance mass, i.e., $M_R \leq M_{\max}$. The energy-momentum conservation in this case is similar to Eq. (3), but with additional constraint that M_1^* in Eq. (6) should satisfy inequality $M_1^* \leq M_{\max}$. For illustrative purposes we choose $M_{\max} = 3.5$ GeV/c^2. The values of M_R, v_R, and $E_\pi^{\max}$ as functions of projectile momentum p_0 are shown in Fig. 14. Almost constant values of v_R and $E_\pi^{\max}$ are observed at large p_0. In fact, v_R is slightly increasing and $E_\pi^{\max}$ slightly decreasing, but this is hardly seen in Figs. 14 (b) and (c), respectively.

B. Comparison with the data in p+A collisions

The UrQMD simulation of p+A reactions were done for most central collisions with zero impact parameter. To compare our results for the pion spectra with available data for the inclusive cross sections in p+A collisions we introduce additional normalization factor considered as a free parameter.

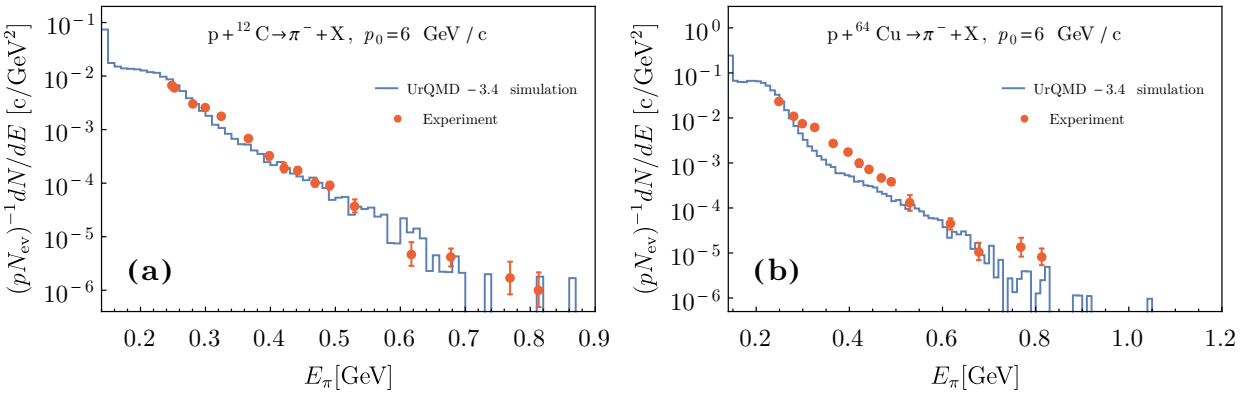

Figure 15: Comparison of the UrQMD results for π^- spectra at 180° with existing data[1] in p+C and p+Cu reactions at p_0=6 GeV/c, $N_{\rm ev} = 10^8$.

In Fig. 15 a comparison of the UrQMD results with the data [1] is shown for reactions p+C$\to \pi^- + X$ (a) and p+Cu$\to \pi^- + X$ (b) at $p_0 = 6$ GeV/c. One may conclude that UrQMD gives a satisfactory description of the shape of energy spectra for $\pi^-(180°)$ at this energy.

More data on cumulative pion production in p+A and A+A reactions at p_0=4.5 GeV/c are presented in Ref. [23], and their analyzes within the FRITIOF model in Refs. [27] and [28].

C. UrQMD analysis of p+A reactions

In this subsection we present the UrQMD simulations for central p+A$\to \pi(180°)$+X collisions and make their microscopic analysis. The total pion spectra summed over all charges will be presented. The UrQMD gives a good opportunity to study a history of each individual reaction. Let us start from the results for p+C reactions at $p_0 = 6$ GeV/c. In Figs. 16 (a) the contributions to $\pi(180°)$ spectrum from the decays of resonances (solid line) and strings (dashed line) are presented.

The resonance contribution is evidently a dominant one. The next question concerns the history of each resonance contributing to the $\pi(180°)$ spectrum. Particularly, how many successive collisions with nuclear nucleons take place? In Fig. 16 (b) we compare the spectra of

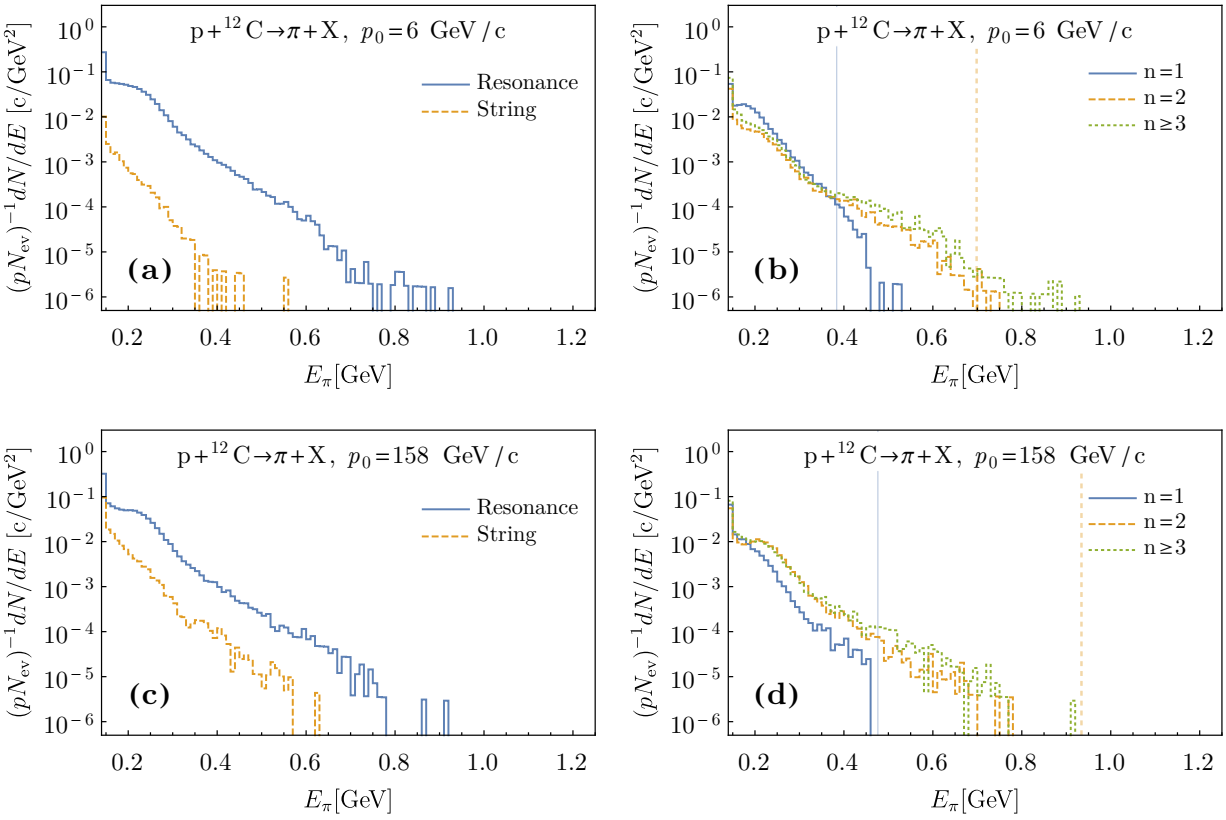

Figure 16: UrQMD results for the pion energy spectra at 180° in p+^{12}C collisions. (a): The solid line presents the total pion spectrum from resonance decays, the dashed line – from the decay of strings. (b): Spectra for pions created after different number of collisions with nuclear nucleons: $n = 1$ (solid line) collision, $n = 2$ (dashed line), and $n \geq 3$ (dotted line). Vertical lines correspond to energies $E^*_{\pi,1}$ (solid) and $E^*_{\pi,2}$ (dashed). In (a) and (b), $p_0 = 6$ GeV/c and the number of events $N_{\rm ev} = 10^9$. (c) and (d): Same as in (a) and (b), respectively, but at $p_0 = 158$ GeV/c with $N_{\rm ev} = 3.8 \cdot 10^7$.

$\pi(180°)$ emitted from resonance decay after $n = 1$ (solid line), $n = 2$ (dashed line), and $n \geq 3$ (dotted line) successive collisions of the projectile with nuclear nucleons. The vertical solid and dashed lines show the values of $E^*_{\pi,1} \cong 0.38$ GeV and $E^*_{\pi,2} \cong 0.70$ GeV in Fig. 16 (b) and $E^*_{\pi,1} \cong 0.48$ GeV and $E^*_{\pi,2} \cong 0.93$ GeV in Fig. 16 (d). These quantities correspond to the kinematical limits for the pion energy emitted at 180° for, respectively, one and two successive collisions with nuclear nucleons at given value of initial momentum p_0.

From Figs. 16 (b) and (d) one observes that E_π may exceed $E^*_{\pi,1}$ even for $n = 1$ contribution. This happens because of nucleon motion inside nuclei (Fermi motion) which exists in the UrQMD model. This effect is, however, not large. The main contribution to the kinematical region forbidden for p+N collisions (i.e., to $E_\pi > E^*_{\pi,1}$) comes from the decays of resonances created within $n = 2$ and $n \geq 3$ successive collisions with nuclear nucleons. These are the

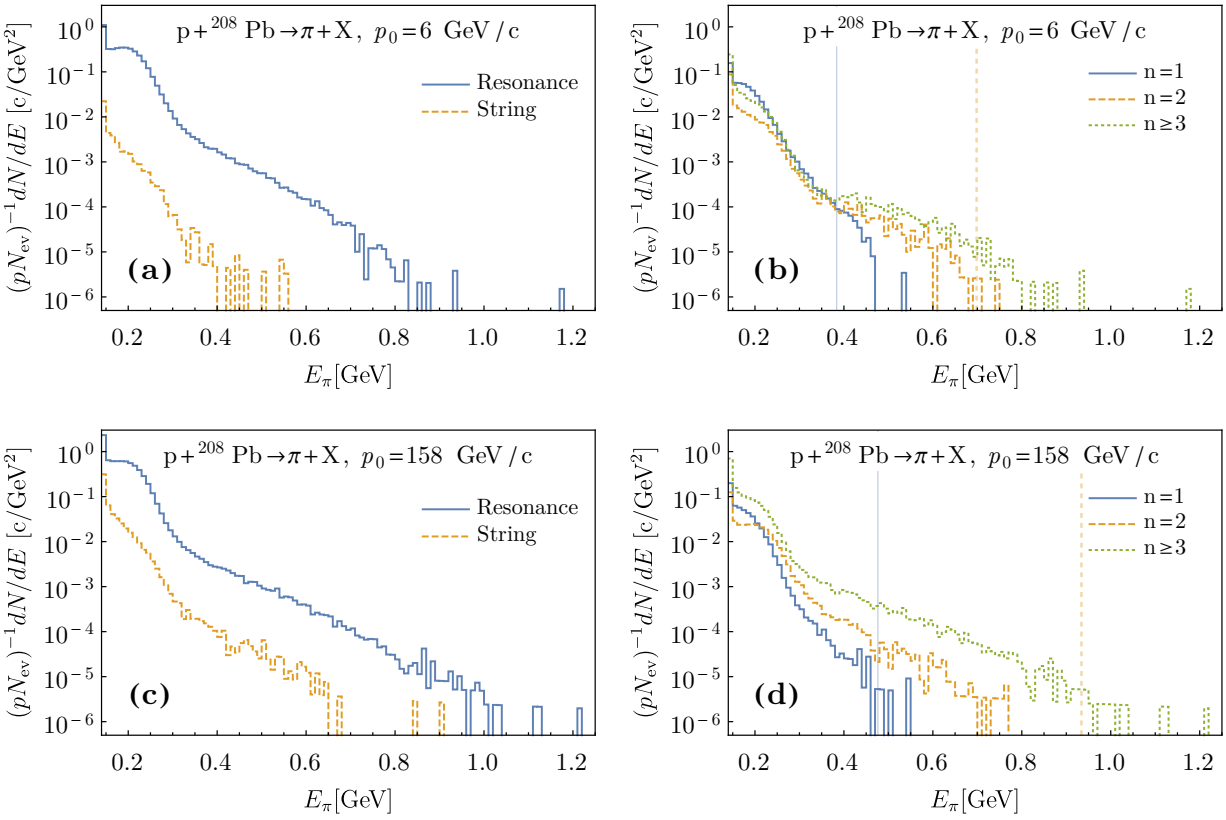

Figure 17: Same as in Fig. 16 but for p+^{208}Pb collisions. (a) and (b): $N_{\rm ev} = 7 \cdot 10^7$. (c) and (d): $N_{\rm ev} = 4.2 \cdot 10^7$.

massive baryonic resonances that are included in the UrQMD model. Note that the role of heavy baryonic resonances within the UrQMD simulations was also discussed in Refs. [29–31].

V. SUMMARY

Pion production in the backward direction in the target rest frame in p+A collisions is considered . Pions created outside the kinematical boundary of p+N reactions are studied. This is the so called cumulative effect discovered in p+A reactions about 40 years ago. We develop the model, where particle production in the cumulative region is due to the formation of massive resonance states, successive collisions of this resonances with nuclear nucleons, and finally their decay with emission of a cumulative particle. The restrictions that follow from energy-momentum conservation are studied. In p+A interactions, the resonances created in p+N reactions may have further inelastic collisions with nuclear nucleons. Due to successive collisions with nuclear nucleons, the masses of these resonances may increase and simultaneously their longitudinal velocities decrease. In our model, these two effects give an explanation of

the cumulative pion production. The simulations of p+A reactions within the UrQMD model support this physical picture.

It should be noted that hadron-like systems with very high masses (heavy resonances, Hagedorn fireballs, quark-gluon bags, baryon and meson strings) are of primary importance for properties of strongly interacting matter at high temperatures and/or baryonic density. They may have also decisive influence on the transition between hadron matter and quark-gluon plasma, and define the type of this phase transition and existence of the QCD critical point itself. However, reliable experimental information about the properties of these heavy hadron-like states, and even about their existence, are absent. We suggest that further experimental studies of cumulative effect in p+A reactions at high collision energies are probably the best way to search for signatures of very heavy hadron-like objects and investigate their properties. Particularly, these studies can be done by the NA61/SHINE Collaboration [32, 33] at the SPS CERN, where the hadron production in p+p, p+A, and A+A collisions is investigated. New efforts may be also required to extend existing relativistic transport models, like UrQMD and HSD, by adding to their formulations string+hadron inelastic reactions that are absent in the present codes of these models.

Acknowledgments

We would like to thank Elena Bratkovskaya, Marek Gaździcki, Volodymyr Vovchenko, and Gennady Zinovjev for fruitful discussions and comments. We are thankful to the staff of the computer maintenance department in Bogolyubov Institute for Theoretical Physics, Kiev for the access to the local cluster computer. The work of M.I.G. was supported by the Program of Fundamental Research of the Department of Physics and Astronomy of NAS.

---

[1] A. M. Baldin *et al.* Yad. Fiz. **20**, 1201 (1974).

[2] A. M. Baldin, Part. Nucl. **8** 429 (1977).

[3] G. A. Leksin, *Proceedings of the 18th International Conference on High Energy Physics, Dubna, 1977, vol.1, AG-3*; V. S. Stavinsky, *ibid.,* AG-1.

[4] S. Frankel *et al.*, Phys.Rev. C **20**, 2257 (1979).

[5] Yu.D. Bayukov *et al.*, Phys.Lett. B **85**, 315 (1979).

[6] V. V. Burov, V. K. Lukyanov, and A. I. Titov, Phys. Lett. B **67**, 46 (1977).

[7] M. I. Gorenstein and G. M. Zinovjev, Phys. Lett. B **67**, 100 (1977).

[8] R. Amado and R. Volosyn, Phys. Rev. Lett. **36**, 1435 (1976).

[9] S. Frankel, Phys. Rev. Lett. **38**, 1338 (1977).

[10] L. L. Frankfurt and M. I. Strikmann, *Proceedings of the Fifth International Conference on High Energy Physics Problems*, Dubna, p. 300 (1978); El. Part. At. Nucl. **11**, 571 (1980); Phys. Rep. **76**, 215 (1981) and **160**, 235 (1988).

[11] V. K. Lukyanov and A. I. Titov, El. Part. At. Nucl. **10**, 815 (1979).

[12] A. V. Efremov, Yad. Fiz. bf 24, 1208 (1976).

[13] A. V. Efremov, A. B. Kaidalov, V. T. Kim, G. L. Lykasov, and N. V. Slavin, Yad. Fiz. bf 47 1364 (1988).

[14] M. A. Braun and V. V. Vechernin, Nucl. Phys. Proc. Suppl. **92**, 156 (2004).

[15] M. I. Gorenstein, V. P. Shelest, and G. M. Zinovjev, Yad. Phys. Lett. **26**, 788 (1977); I. G. Bogatskaya, M. I. Gorenstein, and G. M. Zinovjev, Yad. Phys. **27**, 856 (1978).

[16] I. G. Bogatskaya, C. B. Chiu, M. I. Gorenstein, and G. M. Zinovjev, Phys. Rev. C **22**, 209 (1980).

[17] D.V. Anchishkin, M.I. Gorenstein, and G.M. Zinovjev, Phys.Lett. B **108**, 47 (1982).

[18] E. S. Golubyatnikova, G. A. Shakhanova, and V. L. Shmonin, Acta. Phys. Pol. B **15**, 585 (1984).

[19] B. N. Kalinkin and V. L. Shmonin, Phys. Scripta, **42**, 393 (1990) and **57**, 621 (1998).

[20] L. A. Kondratiuk and V. B. Kopeliovich, JETP Lett. **21**, 40 (1975)

[21] V. B. Kopeliovich, JETP Lett. **23**, 313 (1976); Phys. Rep. **139**, 51 (1986).

[22] M. A. Braun and V. V. Vechernin, J. Phys. G **19**, 517 (1993).

[23] V. K. Bondarev, Phys. Part. Nucl. **28**, 5 (1997).

[24] S.A. Bass *et al.*, Prog. Part. Nucl. Phys. **41**, 255 (1998); M. Bleicher *et al.*, J. Phys. G **25**, 1859 (1999); H. Petersen, M. Bleicher, S.A. Bass, and H. Stöcker, arXiv:0805.0567 [hep-ph].

[25] W. Ehehalt and W. Cassing, Nucl. Phys. A 602 (1996) 449; J. Geiss, W. Cassing, and C. Greiner, Nucl. Phys. A 644 (1998) 107; W. Cassing and E.L. Bratkovskaya, Phys. Rept. 308 (1999) 65.

[26] B. Nilsson-Almqvist and E. Stenlund, Comput. Phys. Commun. 43 (1987) 387.

[27] A. S. Galoyan, G. L. Melkumov, and V. V. Uzhinskij, Yad. Fiz. **65**, 1766 (2002).

[28] A. S. Galoyan, G. L. Melkumov, and V. V. Uzhinskij, arXiv:hep-ph/0201074.

[29] J. Steinheimer and M. Bleicher, J. Phys. G **43**, 015104 (2016).

[30] J. Steinheimer, M. Lorenz, F. Becattini, R. Stock, and M. Bleicher arXiv:1603.02051 [nucl-th].

[31] V. Yu. Vovchenko, D. V. Anchishkin, and M. I. Gorenstein, Nucl. Phys. A **936**, 1 (2015).

[32] M. Gazdzicki, NA61/SHINE Collaboration, J. Phys. G **36**, 064039 (2009).

[33] N. Abgrall, et al., NA61 Collaboration, J. Instrum. **9**, P06005 (2014).